

Aqueous Gel in Sands; a Friend or Foe?

V.N. Georgiannou¹, E-M. Pavlopoulou¹ and F.C. Chortis¹

¹Department of Geotechnical Engineering, National Technical University of Athens, Athens, Greece

E-mail: vngeor@civil.ntua.gr

ABSTRACT: The response of sands stabilized with colloidal silica aqueous gel is examined in the laboratory. The role of colloidal silica on subsequent sand behaviour is examined with the aid of monotonic loading tests to establish the mechanical response and the resistance of the treated sand to liquefaction. It appears that depending on the loading conditions while the strength of the treated sand is enhanced, its stiffness may reduce and its compressibility increase. This contradictory behaviour is investigated on the basis of an extended database including direct shear, triaxial and normal compression tests.

KEYWORDS: Soil stabilization, Laboratory tests, Sands

1. INTRODUCTION

Review of the literature shows that sand stabilized with silica gel shows enhanced strength and liquefaction characteristics compared to untreated sand; in a way reminiscent of structured soils. The influence of microstructure was first recognized by Terzaghi (1941), and Skempton and Northey (1952), proposed the comparison of the response of natural intact and reconstituted clays. Burland (1990), presented a framework based on soil response to normal compression and shearing to assess the enhanced strength and stiffness arising from the microstructure of a structured material compared to its reconstituted state. A response observed repeatedly for a range of soils (e.g. Hight et al., 1992; Allman and Atkinson 1992; Burland et al. 1996; Cotecchia and Chandler 1997; Chandler 2000; Georgiannou and Burland 2001; Mitchell and Soga 2005; Arroyo et al. 2011, Georgiannou et al. 2018).

In this paper, the fundamental behaviour of sands stabilized with colloidal silica aqueous gel is thoroughly examined for a range of loading conditions to verify the robustness of the notion of their enhanced resistance to shearing. Interest in the addition of colloidal silica nanoparticles' solutions in sands, for remediation of their liquefaction potential, is prompted by a new method of 'passive stabilization' proposed in recent years for the mitigation of liquefaction under seismic loading. In this method, a colloidal silica (CS) dilute solution (hydrosol) is introduced in the water regime and transported through the target sand deposit by means of natural or enhanced groundwater flow (Gallagher and Mitchell 2002; Gallagher et al. 2007). The low viscosity hydrosol thickens in a controllable manner to form a stable non-toxic gel; the gel fills the pore space, retains the pore water and supports the grain structure.

Naturally, laboratory studies have been concentrating on undrained cyclic tests to determine the resistance of the treated sand to liquefaction. In most of these studies (Towhata and Kabashima 2001; Gallagher and Mitchell 2002; Kodaka et al. 2005) liquefaction resistance is defined by a threshold strain accumulated during cyclic loading without measurements of generated excess pore water pressure. Other studies resort to simple shear tests under constant volume conditions to eliminate the shortcomings of pore pressure development during undrained loading (Diaz-Rodriguez et al. 2008; Finn and Vaid 1977). Fewer studies report pore pressure measurements during undrained cyclic loading (Porcino et al. 2012; Kodaka et al. 2005). Furthermore, conflicting evidence is presented with respect to loading mode, stress level dependency, cohesive properties of treated sand which is not conclusively addressed.

There is a growing consensus that extreme dilation is associated with stabilized sand often being compared with dense sand albeit its cohesive properties reported in the literature. Georgiannou et al. (2017) observed that the ultimate vertical displacement during testing of medium-dense treated sand in the direct-shear box is much higher than the mean grain size, which was found to be approximately the limiting vertical displacement in the case of dense untreated sand. The

authors regarded the treated sand as a structured material.

The need to incorporate the mechanical behaviour of stabilized sands into a framework, such as that presented by Burland in his seminal 1990 Rankine Lecture, is highlighted herein. To this end, the mechanical behaviour of the untreated sand is first evaluated in the context of critical state theory, and subsequently used as a frame of reference for understanding and interpreting the properties of the stabilized sand. Compressibility and strength properties are investigated to check the robustness of the enhanced microstructure of the stabilized sand under various loading conditions. Drained and undrained tests are performed, at stress levels in the range of 100kPa to 2000kPa. The pore water pressure within the colloidal silica aqueous gel is controlled or measured depending on the drainage conditions, and the results are analyzed in terms of effective stresses; stress-dilatancy relationships and strength parameters at phase transformation (Ishihara et al. 1975), peak and critical state are defined.

2. MATERIALS AND TESTING PROCEDURES

Specimens were prepared from M31 sand, a medium-fine quartz sand, with mean particle diameter $D_{50} = 0.3$ mm, limiting void ratios $e_{min} = 0.528$ and $e_{max} = 0.870$ and specific gravity $G_s = 2.65$. The shape properties and surface characteristics of the sand are reported by Aluhafi et al. (2016) and Georgiannou et al. (2017). The grain size distribution curve of the sand is shown in Figure 1. The water sedimentation method is used to prepare the sand specimens; this method yields uniform and repeatable specimens with a fabric similar to that of natural deposits (Vaid et al. 1999). Treated sand specimens are also formed by sedimentation of the dry sand through a hydrosol.

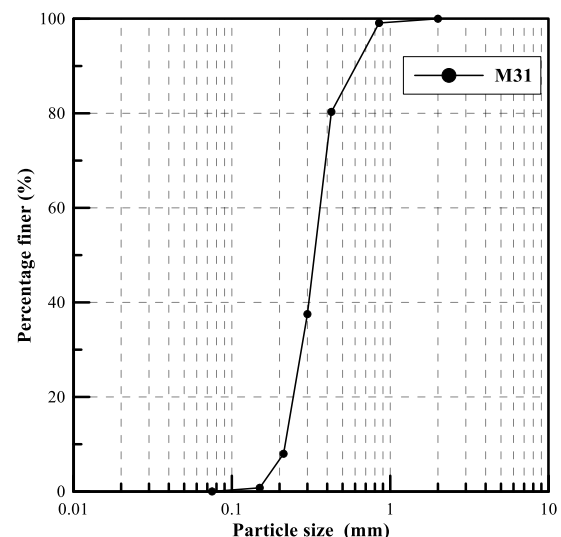


Figure 1 Grain size distribution curve of M31 sand

The hydrosol is a dilute solution of a 10% by weight suspension in water of colloidal-silica (CS) particles, with an average diameter of 7 nm and a specific surface of 320-400 m²/g; obtained by adding distilled water to a supplied concentrated 30 wt. % suspension (Ludox SM-30) with a pH of around 10, a density of 1.22 g/cc (at 25 °C) and a dynamic viscosity of around 5.5 cP (1cP=1 mPa.s). The dilute (10 wt. %) silica hydrosol has viscosity little above 1 cP (1 cP=1 mPa.s); electrolyte (NaCl) and acid (HCl) are also added to adjust its ionic strength to a value of 0.03 N, and the PH level to 6. Under these conditions, the sol thickens quickly as the colloidal particles collide and siloxane bonds are formed. The gel time is defined as the time needed for the viscosity to rise above 100 cP and was calculated to be 10 h (Agapoulaki et al. 2015).

After 50 hours of curing in isolated conditions at room temperature, the colloidal hydrosol forms a gel allowing handling of the specimen. In triaxial tests, the prepared treated specimens are formed to the target density, similar to that of untreated sand, in split moulds of 50 mm diameter and 100 mm height. In the case of direct shear, the samples were 60 mm in diameter and approximately 24 mm in height. Specimens for oedometer tests are formed within the apparatus.

The testing programme included: i) direct shear tests on treated and untreated M31 sand for a range of normal stresses, $\sigma_v=125-555$ kPa, and void ratios, $e_i=0.550-0.656$. ii) Drained and undrained triaxial compression tests on treated and untreated M31 sand, at initial effective stresses, p' , ranging from 100 to 2000 kPa. Tests were carried out in computer-controlled Bishop and Wesley (1975) triaxial stress path cells with an accuracy of ± 0.5 kPa in pressure and ± 0.1 N in load measurements. Submersible linear variable differential transducers (LVDTs) were mounted diametrically opposite over a central axial gauge length of the specimens. Drained tests on stabilized sand were performed under a range of back pressures (300 to 700 kPa) and the results are found to be independent of the magnitude of back pressure, indicating that increased pore water pressure does not induce damage to the gel; the undrained tests were performed at an initial pore water pressure of 700 kPa to avoid cavitation as shearing advances towards critical state at strains around 30%. A variation in the imposed shearing rate between 0.005 to 0.050 mm/min did not affect the results; Shearing rates of 0.005 and 0.025 mm/min were applied on specimens with rough end platens. Critical states were obtained for specimens, failing mainly by bulging, under practically constant stresses, q and p' , with increasing shear strain, without considerable plastic volumetric and/or excess pore water pressure changes. iii) Normal compression loading tests on M31 silica treated sand, to assess its compressibility with reference to untreated sand.

3. RESULTS AND DISCUSSION

3.1 Monotonic loading tests

The response of stabilized M31 sand has been compared to that of untreated M31 sand by Georgiannou et al. (2017) who observed that the behaviour of the treated sand differs in important respects from the behaviour of the untreated sand: a significant increase in the angle of shearing resistance is observed at lower stress levels diminishing with increasing stress level; the stress ratio at peak strength, τ/σ_v' , is significantly higher for the treated sand at medium density than the untreated sand at the same density while at ultimate strength the stress ratios coincide for treated and untreated sands. However, at all stress levels extreme dilation is associated with the treated sand at peak and ultimate strength conditions, diminishing only at the highest stress level considered herein.

In Figure 2 the strength envelopes for treated sand show negligible apparent cohesion intercept, while the angle of shearing resistance is stress level dependent with a value of $\phi_p=41.3^\circ$ at $\sigma'_{v0}=125$ kPa and $\phi_p=34.9^\circ$ at higher stress levels, compared with $\phi_p=32.5^\circ$ observed for untreated sand. At peak strength conditions the frictional characteristics of the treated sand tend to those of the untreated sand as stress and strain level increases while at ultimate

strength they coincide indicating weak bonding.

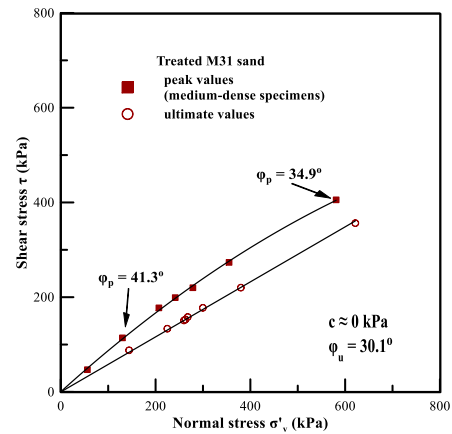


Figure 2 Strength envelopes for treated M31 sand: peak and ultimate strength conditions in direct shear tests

Figure 3 is reproduced from these data, included in Table 1, and obtained from highly repeatable treated sand specimens as reported by Georgiannou et al. 2017. Figure 3 shows the stress level dependency which may be associated with destructuration and is a characteristic response of the treated sand only. After initial contraction, at comparable levels with the sand, the treated sand exhibits extremely high dilatancy rates at peak strength; dilating towards ultimate strength by more than four times compared to the untreated sand's specimens. This enhanced dilation has been consistently observed in the literature where the treated loose sand is considered as equivalent to dense untreated sand (Porcino, 2012).

A dense sand specimen, shown as a broken line in Figure 3, exhibits a lower dilatancy rate and final volume change than the treated specimen despite the initial contraction of the latter due to its lower density. It is interesting to note that the ultimate vertical displacement of the treated sand is significantly higher than the mean grain size, which was found to be approximately the limiting displacement in the case of the dense untreated sand; indicating that the stability and kinematics of the grain structure inside the shear band, which determine the ultimate void ratio (Cassagrande and Watson 1938; Roscoe 1970; Vardoulakis and Sulem 1995; Desrues et al. 1996; Wang and Leung 2008; Fu and Dafalias 2011), differ significantly for the treated and untreated sand despite being sheared at the same ultimate stress ratio towards critical states.

Table 1 Direct Shear Tests

Test	e_i	e_p	σ'_{v0}	τ/σ'_v
M-1	0.641	0.638	125	0.665
M-2	0.656	0.655	555	0.630
M-3	0.550	0.542	125	0.766
M-4	0.535	0.524	125	0.758
M-5	0.651	0.646	232	0.641
M-6	0.661	0.656	232	0.612
M-7	0.528	0.523	232	0.749
M-8	0.626	0.618	232	0.729
M-9	0.658	0.653	340	0.650
M-10	0.696	0.696	125	0.587
M-11	0.554	0.547	555	0.742
SM-1	0.639	0.623	125	0.877
SM-2	0.632	0.625	555	0.698
SM-3	0.637	0.619	196	0.857
SM-4	0.647	0.631	232	0.824
SM-5	0.612	0.600	232	0.884
SM-6	0.643	0.625	268	0.789
SM-7	0.646	0.623	340	0.770
SM-8	0.681	0.676	340	0.723
SM-9	0.655	0.621	53	0.835

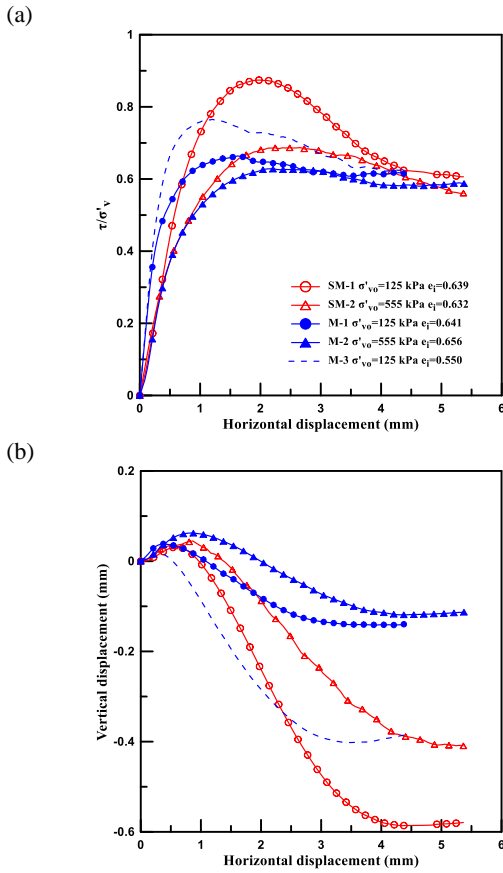


Figure 3 Direct shear tests on treated and untreated M31 sands: (a) stress ratio τ/σ'_v against horizontal displacement curves; (b) vertical displacement against horizontal displacement curves

The observations made under direct shear loading are supported by the drained triaxial tests on treated and untreated M31 sand, shown in Figure 4(a) in terms of stress ratio, $\eta=q/p'$, against axial strain for a range of confining stresses from 100 kPa to 700 kPa. Test details are described in Table 2. The treated sand exhibits stress level dependency with the peak stress ratio decreasing with stress contrary to untreated sand which attains the same, lower bound, stress ratio at peak depending only on density. The same ultimate strength is approached by both treated and untreated sands at large strains, albeit the nearly fivefold increase in dilation exhibited by the treated sand specimens shown as broken lines in Figure 4(d), as observed earlier in Figure 3(b). It appears that the support provided by the CS aqueous gel at interparticle and intrapore level diminishes continually with stress and strain level rendering stress ratios similar to the sand's; yet the gel precipitates dilation by forcing the grains and/or the grain gel clusters to rearrange to a looser state with shearing pertaining up to the ultimate state, at least in the range of low and medium stress levels.

To assess the role of the gel in setting the structure of stabilized sand, typical stress dilatancy relationships are shown for the treated and untreated M31 sand under direct shear at 125 kPa and triaxial loading at 700 kPa; the former expressed as $D=dy/d\chi$ against τ/σ'_v and the latter as $D = d\epsilon_{vol}/d\epsilon_a$ against q/p' in Figure 5 (a) and (b) respectively. The peak stress ratio and maximum dilatancy occur simultaneously indicating a lack of interparticle cementation bonding (Cuccovilio and Coop 1999). Additionally, contrary to stabilized sands, cemented sands exhibit different ultimate strengths than their untreated counterparts (Wang and Leung 2008). Mitchell (1976) defined as 'structure' the combination of fabric and interparticle bonding. It follows that it is the fabric - commonly expressing the shape and packing of particles as well the orientational distribution of contact normals and, particle and pore space directions - modified by the presence of gel at an interparticle and intrapore level that controls the behaviour of the sands stabilized with colloidal silica gel, rather than bonding.

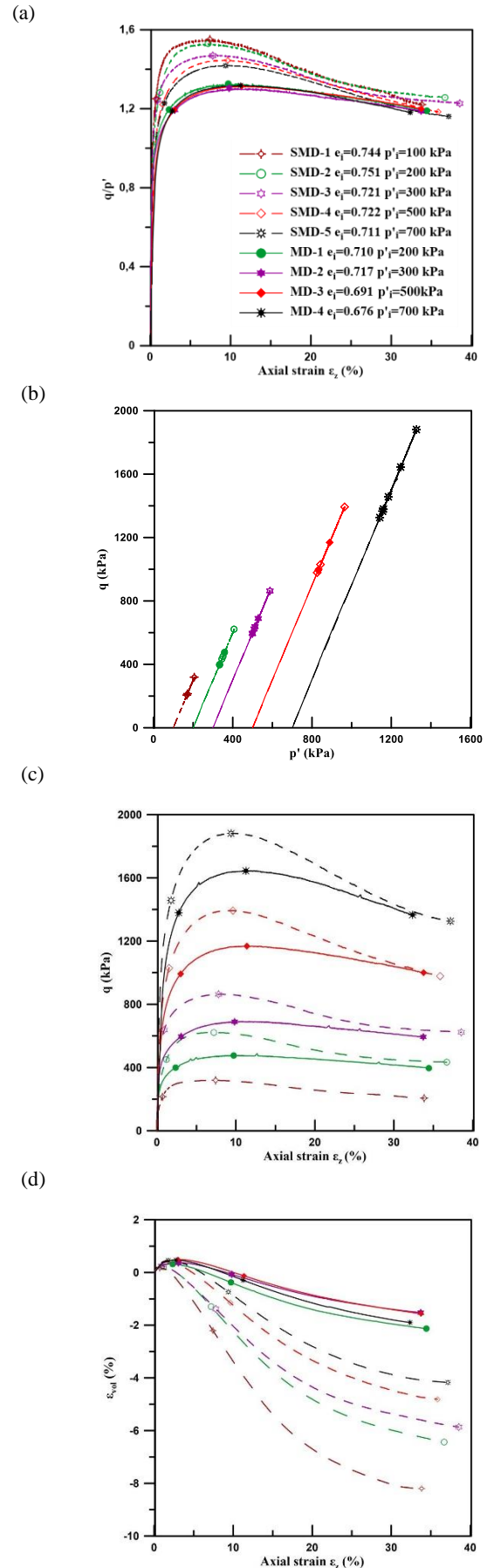


Figure 4 Drained triaxial tests on treated and untreated M31 sands: (a) stress ratio q/p' against axial strain curves; (b) effective stress paths; (c) stress-strain curves; (d) volumetric strain against axial strain curves

The study of fabric is beyond the scope of this paper however, in the micrographs of the optical microscope shown in Figure 7(a) for treated sand specimens, the presence of hydrogel at interparticle contacts can be identified. In Figure 7(b) the air-dried xerogel can be contrasted with the hydrogel in Figure 7(a); the former being cracked due to inhomogeneous shrinkage induced stresses, the latter maintaining the capacity to absorb and/or discharge free water during mechanical loading.

Figure 6 (a,b,c) shows the results of undrained tests, in terms of effective stress paths in the $q-p'$ plane, stress-strain curves in the $q-\epsilon_z$ plane and plots of excess pore-water pressure ratio $\Delta u/p'$ against ϵ_z . Excess pore water pressure is normalized with respect to initial mean effective stress, p'_i . Solid and hollow symbols and solid and dashed lines are used for the untreated and treated sand respectively. The symbols in Figure 6 as well as in Figure 4 referring to the drained tests indicate, in the order of appearance, the phase-transformation points (PTPs), the peak- η failure states ($\eta = q/p'$) and the states at the end of testing, which may or may not be critical states.

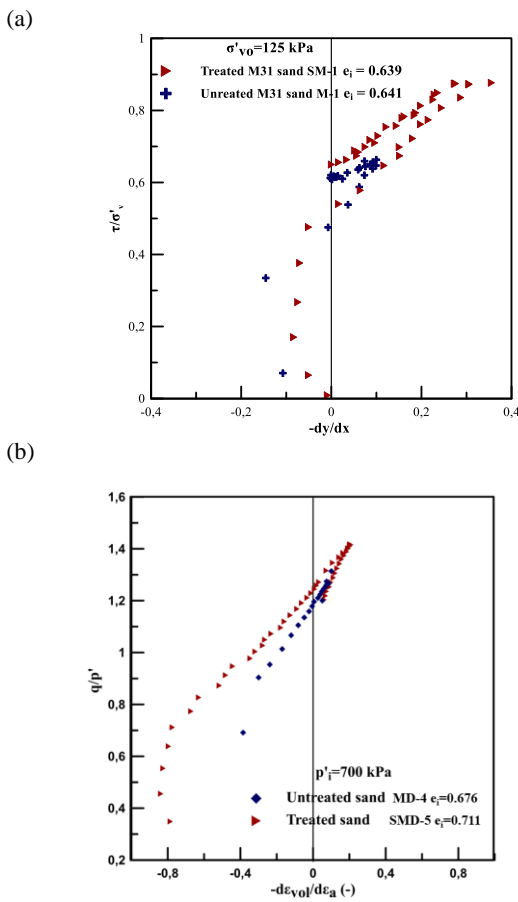


Figure 5 Stress-dilatancy curves for treated and untreated M31 sands: (a) direct shear tests; (b) drained triaxial tests

Figures 4c and d show a steady increase in drained strength, which is attained at lower strain, at phase transformation, q_{PT} , and peak state q_p for treated compared to untreated sand, consolidated to the same mean effective stress and similar density, while the ultimate drained strength q_{ult} is common for treated and untreated sand specimens. Volumetric strain accumulation is also lower at phase transformation, however, comparable contractant behaviour is evidenced for all specimens with differences arising as dilation builds up at a significantly increased rate for the treated sand in Figure 4d. The increase in consolidation stress induces a gradual decrease in the peak dilatancy rate and ultimate dilation for the treated sand, also reported by Georgiannou et al. (2017). The undrained behaviour (Figures 6a to c) of treated sand follows the trends set under drained loading. Due to high dilative tendencies cavitation is induced despite the high value (700 kPa) of initial pore

water pressure, hence tests SMU-1, SMU-2 & SMU3 did not reach their ultimate strength. The differences in the tendency for dilation, reflected by the evolution of $\Delta u/p'_i$ in Figure 6c, are more pronounced at low stresses yet they still exist at stresses as high as 2000 kPa.

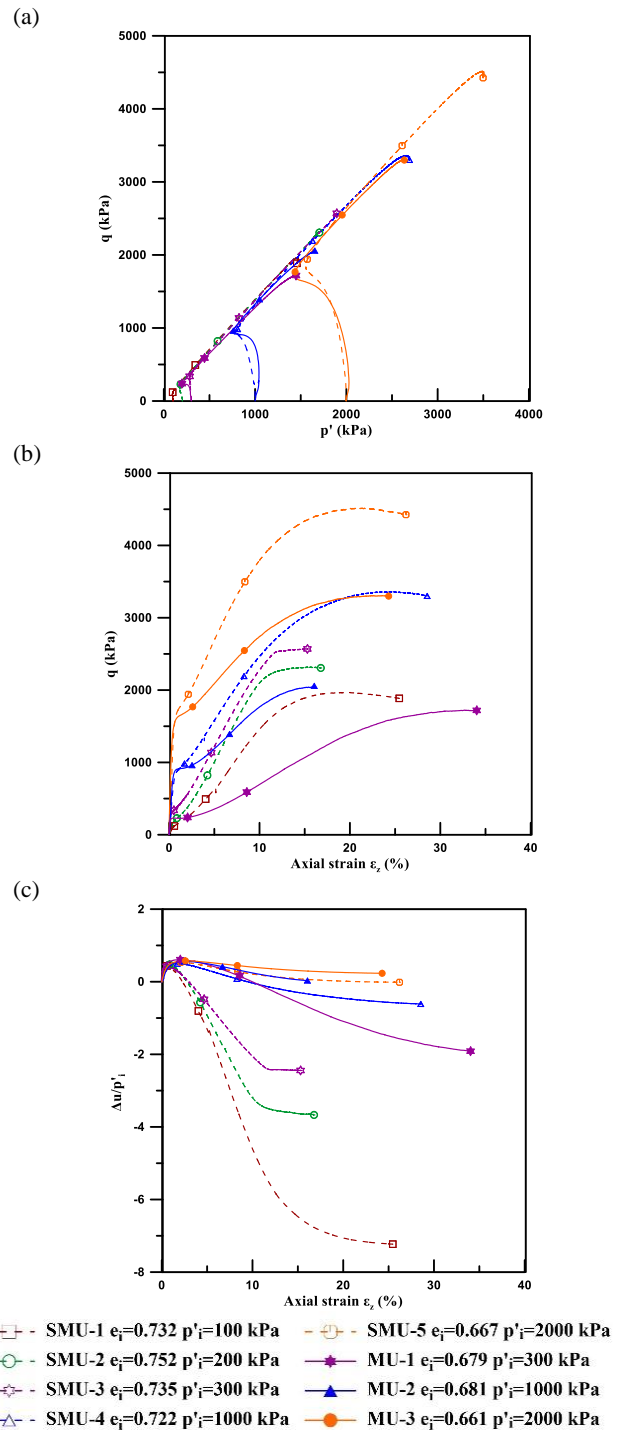


Figure 6 Undrained triaxial tests on treated and untreated M31 sands: (a) effective stress paths; (b) stress-strain curves; (c) excess pore-water pressure ratio against axial strain curves

Figure 8 shows the critical states of untreated and treated M31 sand, respectively, in the state diagram $e-p'$, determined from both drained and undrained triaxial tests. The position of the critical state line for the treated sand reflects the extreme dilation associated with the structure of the treated sand which is rearranged to a looser state with shearing up to the ultimate state. At high stresses, dilation is suppressed and the two lines converge. Despite the difference in

critical void ratio a common ultimate stress ratio $M=1.24$ ($\phi_{cs}=30.9^\circ$) is attained by treated and untreated sand, indicating that stabilization does not enhance ultimate shear resistance above that of mineral-to-mineral friction and constant-volume remoulding (Rowe 1962).

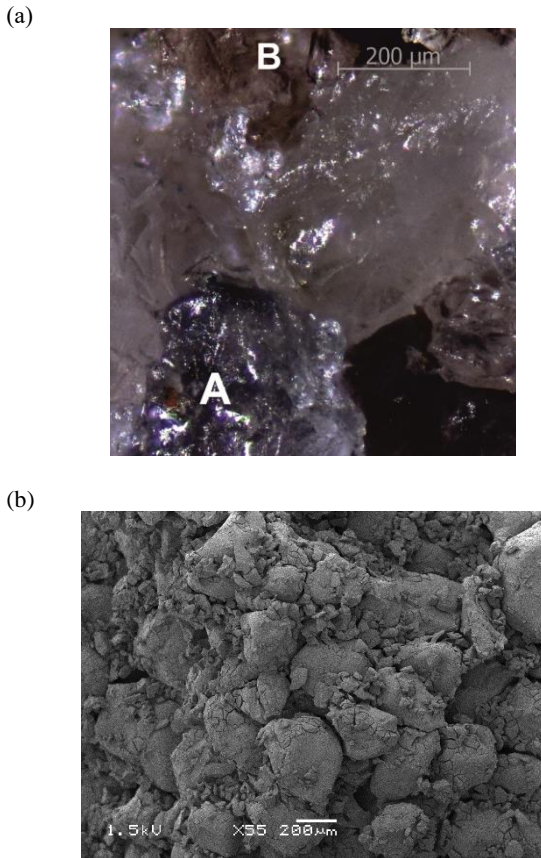


Figure 7 Optical micrographs showing treated sand specimens in (a) wet and (b) dry conditions

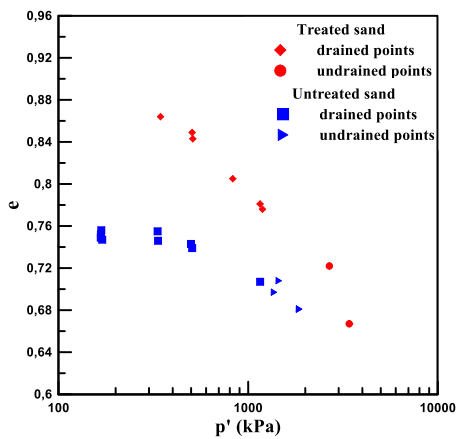


Figure 8 Critical states of untreated and treated M31 Sand

The effect of stabilization in the initial stage of shearing, before phase transformation, appears also to diminish, as discussed in Figures 4(d) and 6(c) where both treated and untreated sands show a contractant phase. These results are also supported by the normal compression tests presented next.

Kodaka et al. (2005) performed cyclic torsional shear tests on silica treated and untreated Toyoura sand. The latter initially develops small strains and as pore water pressures accumulate the effective stress path migrates close to the phase transformation line, PTL, defined under monotonic loading conditions; in the vicinity of the PTL unstable behaviour leading to liquefaction is introduced. This is a common characteristic of stable (non-brittle) sands under

monotonic loading also reported by Georgiannou et al. 2008, Georgiannou and Tsomokos 2008. However, the treated sand shows a very soft response under cyclic loading with large strains developing from the very first cycle and pertaining through cyclic loading in the range between -4% and 3%. Despite this weakness, the treated sand specimens did not collapse and/or liquefied. Similar behaviour is reported for treated sand by Porcino et al. (2011).

Table 2 Triaxial Tests

Test	Test Type	e_i	p'_i	Treated
MD-1	D	0.710	200	-
MD-2	D	0.717	300	-
MD-3	D	0.691	500	-
MD-4	D	0.676	700	-
SMD-1	D	0.744	100	T
SMD-2	D	0.751	200	T
SMD-3	D	0.721	300	T
SMD-4	D	0.722	500	T
SMD-5	D	0.711	700	T
MU-1	U	0.679	300	-
MU-2	U	0.681	1000	-
MU-3	U	0.661	2000	-
SMU-1	U	0.732	100	T
SMU-2	U	0.752	200	T
SMU-3	U	0.735	300	T
SMU-4	U	0.722	1000	T
SMU-5	U	0.667	2000	T

D, drained triaxial test; U, undrained triaxial test; T, treated specimen

3.2 Normal compression tests

Georgiannou et al. (2017), reported that while isotropic compression induces similar deformations for treated and untreated sand, normal compression loading in the oedometer results to significantly increased vertical deformations for the treated sand only. This weakness of the treated sand under anisotropic compression loading is further investigated for a range of densities for M31 treated and untreated sands. The results are presented in Figure 9. Solid and hollow symbols are used for the untreated and treated sand respectively. The results show that: i) at the same density normal compression induces higher volume changes in the treated compared to untreated sand and ii) this trend is consistent at low and high densities.

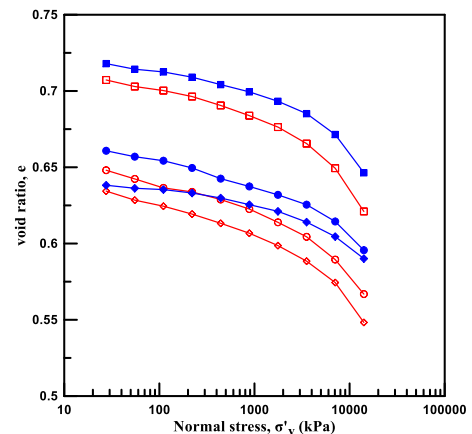


Figure 9 1D compression Tests

The high potential of the colloidal silica to absorb water reported by Bergna and Roberts (2005), was evidenced in the dilatant phase of shearing; the aqueous gel (hydrogel) in response to the structural rearrangement imposed during shearing absorbs water available in drained tests and the treated sand specimens show extreme dilation. When rapidly compressed under drained conditions in the oedometer, the compression curves of the treated sand show curvature as they

depart from the corresponding curves of the untreated sand with increasing stress level; a sign of structural breakdown. It has been reported in the literature that the aqueous gel can be easily damaged albeit its self-healing ability (Brinker and Scherer 1990; Vigil et al. 1994); it can be inferred that during normal compression the gel is being damaged and free water is pushed out of the pores. When yielding has fully developed at a high stress level the treated sand has attained its densest state similar to e_{min} . Interestingly, the untreated sand shows lower densification at the same stress level as if slippage of the sand grains is facilitated in the presence of the gel.

3. CONCLUSION

The beneficial effect of stabilizing medium density and loose sands with colloidal silica gel in increasing liquefaction resistance and mitigating liquefaction under seismic loading is supported by literature and evidenced in this experimental investigation. It is shown that the treated sand can be regarded as a structured material lacking bonding.

However, stabilization by means of chemical grouting using colloidal silica hydrosol is not the panacea for all ills of liquefiable deposits. Under drained and undrained loading there is no significant improvement in the tendency for contraction of loose untreated sand. Furthermore, under normal compression, the treated sand shows significantly higher volumetric changes compared to untreated sand. These findings are corroborated by cyclic loading tests reported in the literature, with the treated sand accumulating strain and excess pore water pressure faster than the untreated sand.

The above features have multiple implications for the effect of stabilization which in turn determines the effectiveness of the method of 'passive stabilization'.

4. ACKNOWLEDGEMENTS

"This research is carried out / funded in the context of the project "Experimental investigation of the anisotropic behaviour of sand before and after stabilization" (MIS 5049187) under the call for proposals "Researchers' support with an emphasis on young researchers- 2nd Cycle". The project is co-financed by Greece and the European Union (European Social Fund- ESF) by the Operational Programme Human Resources Development, Education and Lifelong Learning 2014-2020."

5. REFERENCES

- Agapoulaki G. I., and Papadimitriou A. G. (2015) "Rheological properties of colloidal silica as a means for designing passive stabilization of liquefiable soils". In Proceedings: XVI European Conference on Soil Mechanics and Geotechnical Engineering (Winter MG, Smith DM, Eldred PJL and Toll DG (eds)). Institution of Civil Engineers, London, UK, vol. 5, pp 2331–2336.
<http://dx.doi.org/10.1680/ecsmge.60678.vol5.356>.
- Allman, M. A., and Atkinson J. H. (1992) "Mechanical properties of reconstituted Bothkennar clay". *Geotechnique* 42 (2), pp 289–301.
<https://doi.org/10.1680/geot.1992.42.2.289>.
- Altuhaifi, F. N., Coop, M. R., and Georgiannou, V. N. (2016) "Effect of particle shape on the mechanical behaviour of natural sands". *Journal of Geotechnical and Geoenvironmental Engineering*, 142(12): 0401671.
- Arroyo, M., Ciantia M., Castellanza R., and Gens A. (2011) "A soft-rock model for cement-improved clays". In Proc., 15th European Conf. on Soil Mechanics and Geotechnical Engineering: Geotechnics of Hard Soils-Weak Rocks. edited by A.Anagnostopoulos, M.Pachakis, and C.Tsatsanifos. 501–506. Athens, Greece: IOS Press.
- Bergna H. E., and Roberts W. O. (eds) (2005) "Colloidal Silica: Fundamentals and Applications". CRC, Boca Raton, FL, USA.
- Brinker C. J., and Scherer G. W. (eds) (1990) "Sol-Gel Science: the Physics and Chemistry of Sol-Gel Processing". Academic Press, Cambridge, MA, USA.
- Burland J. B. (1990) "On the compressibility and shear strength of natural clays". *Geotechnique* 40:3, pp 329-378.
- Burland, J. B., Rampello S., Georgiannou V. N., and Galabresi G. (1996) "A laboratory study of the strength of four stiff clays". *Geotechnique* 46 (3), pp 491–514.
<https://doi.org/10.1680/geot.1996.46.3.491>.
- Casagrande, A., and Watson, J. D. (1938) "Compaction tests and critical density investigations of cohesionless materials for Franklin Falls Dam, Merrimack Valley flood control". Corps of Engineers, U.S. Army Engineering Office, p. BII-7
- Chandler, R. J. (2000) "Clay sediments in depositional basins: The geotechnical cycle". *Q. J. Eng. Geol. Hydrogeol.* 33 (1), pp 7–39. <https://doi.org/10.1144/qjgeh.33.1.7>.
- Cotecchia, F., and Chandler R. J. (1997). "The influence of structure on the pre-failure behaviour of a natural clay". *Geotechnique* 47 (3), pp 523–544.
<https://doi.org/10.1680/geot.1997.47.3.523>.
- Cuccovillo T., and Coop M. R. (1999) "On the mechanics of structured sands." *Geotechnique* 49(6), pp 741–760.
<http://dx.doi.org/10.1680/geot.1999.49.6.741>.
- Desrues, J., Chambon, R., Mokni, M., and Mazerolle, F. (1996) "Void ratio inside shear bands in triaxial sand specimens studied by computed tomography", *Geotechnique* 46 (3), pp 529-546
- Díaz-Rodríguez J. A., Antonio-Izarraras V. M., Bandini P., and López-Molina J. A. (2008) "Cyclic strength of a natural liquefiable sand stabilized with colloidal silica grout". *Canadian Geotechnical Journal*, 45(10), pp 1345–1355.
<http://dx.doi.org/10.1139/T08-072>.
- Finn W. D. L., and Vaid Y. P. (1977) "Liquefaction potential from drained constant volume cyclic simple shear tests". In Proceedings of the 6th World Conference on Earthquake Engineering. Sarita Prakashan, Meerut City, India, vol. 6, pp. 7–12.
- Fu, P., and Dafalias, Y. F. (2011) "Fabric evolution within shear bands of granular materials and its relation to critical state theory". *International Journal for Numerical and Analytical Methods in Geomechanics*, 35, pp 1918-1948.
- Gallagher P. M., and Mitchell J. K. (2002) "Influence of colloidal silica grout on liquefaction potential and cyclic undrained behavior of loose sand". *Soil Dynamics and Earthquake Engineering* 22(9–12), pp 1017–1026.
[http://dx.doi.org/10.1016/S0267-7261\(02\)00126-4](http://dx.doi.org/10.1016/S0267-7261(02)00126-4).
- Gallagher P. M., Conlee C. T., and Rollins K. M. (2007) "Full-scale field testing of colloidal silica grouting for mitigation of liquefaction risk". *Journal of Geotechnical and Geoenvironmental Engineering*, 133(2), pp 186–196.
[http://dx.doi.org/10.1061/\(ASCE\)1090-0241\(2007\)133:2\(186\)](http://dx.doi.org/10.1061/(ASCE)1090-0241(2007)133:2(186)).
- Georgiannou, V. N., and Burland J. B. (2001) "A laboratory study of post-rupture strength". *Geotechnique*, 51 (8), pp 665–675.
<https://doi.org/10.1680/geot.2001.51.8.665>.
- Georgiannou V. N., and Tsomokos A. (2008) "Comparison of two fine sands under torsional loading". *Canadian Geotechnical Journal*, 45(12), pp 1659–1672.
<http://dx.doi.org/10.1139/T08-083>.
- Georgiannou V. N., Tsomokos A., and Stavrou K. (2008) "Monotonic and cyclic behaviour of sand under torsional loading". *Geotechnique*, 58:2, pp 113-124.
- Georgiannou, V.N., Pavlopoulou E. M., and Bikos, Z. (2017) "Mechanical behaviour of sand stabilised with colloidal silica". *Geotechnical Research*, 4(1), pp 1-11.
- Georgiannou V. N., Coop M., Altuhafi F., and Lefas D. (2018) "Compression and Strength Characteristics of Two Silts of Low and High Plasticity". *Journal of Geotechnical and Geoenvironmental Engineering*, 144, Issue 7, 04018041.
[https://doi.org/10.1061/\(ASCE\)GT.1943-5606.0001891](https://doi.org/10.1061/(ASCE)GT.1943-5606.0001891)
- Hight, D. W., Bond A. J., and Legge J. D. (1992). "Characterization of the Bothkennar clay: An overview". *Geotechnique*, 42 (2), pp 303–347.

- <https://doi.org/10.1680/geot.1992.42.2.303>.
- Ishihara, K., Tatsuoka, F., and Yasuda, S. (1975) "Undrained deformation and liquefaction of sand under cyclic stresses". *Soils and Foundations*, Vol.15, No.1, pp 29-44.
- Kodaka T., Oka F., Ohno Y., Takyu T., and Yamasaki N. (2005) "Modeling of cyclic deformation and strength characteristics of silica treated sand". In *Geomechanics: Testing, Modeling, and Simulation* (Yamamuro JA and Koseki J (eds)). American Society of Civil Engineers, Reston, VA, USA, Geotechnical Special Publication 143, pp 205–216.
- Mitchell, J. K., and Soga K. (2005) "Fundamentals of Soil Behavior". 3rd ed. Hoboken, NJ: Wiley.
- Porcino D., Marcianò V., and Granata R. (2011) "Undrained cyclic response of a silicate-grouted sand for liquefaction mitigation purposes". *Geomechanics and Geoengineering: an International Journal*, 6(3), pp 155–170. <http://dx.doi.org/10.1080/17486025.2011.560287>.
- Porcino D., Marcianò V., and Granata R. (2012) "Static and dynamic properties of a lightly cemented silicate-grouted sand". *Canadian Geotechnical Journal*, 49(10), pp 1117–1133. <http://dx.doi.org/10.1139/T2012-069>.
- Roscoe, K. H. (1970) "The influence of strains in soil mechanics". Tenth Rankine Lecture, *Géotechnique* 20, No. 2, pp 129-170.
- Rowe, P. W. (1962) "The stress-dilatancy relation for static equilibrium of an assembly of particles in contact". *Proc. R. Soc. Lond. A*, 269, pp 500-527.
- Skempton, A. W., and Northey, R. D. (1952) "The Sensitivity of Clays". *Geotechnique*, 3, pp 30-53. <http://dx.doi.org/10.1680/geot.1952.3.1.30>
- Terzaghi, K. (1941) "Undisturbed clay samples and undisturbed clays". *J. Boston Sot. Civ. Engrs*, 28(3), pp 45-65.
- Towhata I., and Kabashima Y. (2001) "Mitigation of seismically – induced deformation of loose sandy foundation by uniform permeation grouting". *Proceedings of the Fifteenth International Conference on Soil Mechanics and Geotechnical Engineering, Earthquake Geotechnical Engineering Satellite Conference, Istanbul, Turkey*, pp 313–318.
- Vaid Y., Sivathayalan S., and Stedman D. (1999) "Influence of specimen reconstituting method on the undrained response of sand". *Geotechnical Testing Journal*, 22, 3, pp 187-195.
- Vardoulakis, I., and Sulem, J. (1995) "Bifurcation analysis in geomechanics". Chapman and Hall.
- Vigil G., Xu Z., Steinberg S., and Israelachvili J. (1994) "Interactions of silica surfaces". *Journal of Colloid and Interface Science*, 165, Issue 2, pp 367-385. <https://doi.org/10.1006/jcis.1994.1242>
- Wang, Y. H., and Leung, S. C. (2008) "Characterization of cemented sand by experimental and numerical investigations". *Journal of Geotechnical and Geoenvironmental Engineering*, Vol. 134, No. 7, pp 992-1004.